Journal of
MECHANICAL and ENERGY
ENGINEERING

ISSN: 2544-0780 | e-ISSN: 2544-1671
Vol. 2(42) | No. 2 | June 2018 | pp. 155-162
DOI: 10.30464/jmee.2018.2.2.155

ON THE ENERGY EFFICIENCY IN THE HEATPROOF NOZZLE OF THE PNEUMATIC PULSATOR SYSTEM DURING SUPERSONIC AIRFLOW

Krzysztof J. WOŁOSZ[1*], Jacek WERNIK[1]

[1*] Warsaw University of Technology, Faculty of Civil Engineering, Mechanics and Petrochemistry, Institute of Mechanical Engineering, Łukasiewicza 17, 09-400 Płock, Poland, e-mail: krzysztof.wolosz@pw.edu.pl

(Received 12 April 2018, Accepted 28 May2018)

Abstract: In this article, a study of supersonic airflow through a channel with various cross-section is presented. The channel is namely a heatproof nozzle which is used in a pneumatic pulsator system. The system utilizes a pneumatic impact to destruct or to avoid of the creation of unfavourable phenomena which comes from cohesion forces. The pneumatic pulsator system is driven by compressed air and a high-velocity airflow is induced by the difference between internal and external air pressure. This flow changes its characteristics during a work cycle of the pulsator from subsonic to supersonic conditions. It causes a very dynamic gas conversion and may produce additional heat inside the pulsator and its nozzle. The article presents a method for calculating the value of the heat which can be generated inside the heatproof nozzle. The results of the study shows that the small amount of energy is lost during the airflow which can generate an increment of heatproof nozzle wall temperature.

Keywords: energy efficiency, supersonic airflow, nozzle, transient analysis, pneumatic pulsator

1. INTRODUCTION

The article considers the energy efficiency of a process of compressible airflow though the heatproof nozzle. The nozzle is an industrially applicable equipment and it is a part of a pneumatic pulsator system. The basic goal of the study is to determine the amount of energy which is lost in the nozzle during one work cycle of the system. For that purpose, results of numerical simulation are used.

Pneumatic pulsators are used mostly in heavy industry silos which store bulk and loose materials. The basic function of the pulsators is to avoid an unfavourable phenomena in these materials such as: clinging, bridging, ratholing, and arching. The adverse phenomena cause stoppages in transportation lines and may pose danger to the personnel. They are specific for loose materials and are formed while cohesion forces are larger than the gravity. In order to prevent the bulk material bed from the occurrence of the adverse phenomena, a pneumatic impact is often utilized. Pneumatic pulsators transform energy, which is accumulated in compressed air, to produce the pneumatic impact which acts directly onto the loose material bed and prevents the cohesion forces from increasing. In practice, an air blast hits the loose material bed, crushes the unfavourable structure and moves the material towards the outlet of the silo.

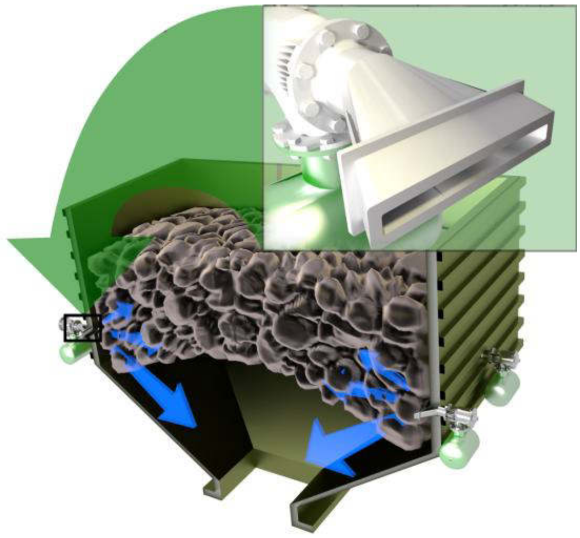

Fig. 1. Pneumatic pulsator system location on a silo walls with heatproof nozzle zoomed

It is common to name pneumatic pulsators as “air cannons” or “air blasters” due to the impact and its source.

Most pulsators are provided with a sort of auxiliary nozzles which, in general, protect the head of the pulsator from the heat which could be generated within the silo. The nozzles are the last element of the pneumatic pulsator system and they often have direct contact with the loose material. Of course, they can also be utilized to direct the airflow in a specific direction. In numerous applications, both tasks are combined. One of this type of the heatproof nozzles is the subject being investigated herein.

The heat from the silo can be generated directly from the loose material which comes from an industrial furnace. Its temperature generates heat within this silo which affects the pulsator directly. Therefore, it is recommended to apply to the pneumatic pulsator system a heatproof nozzle. Furthermore, the airflow through the pulsator is thermodynamic gas conversion which during the compression may produce additional heat and causes failure for the pulsator or the nozzle eventually. Hence, the aim of this study is to develop a method for the calculation of the amount of heat during one work cycle.

Many researches have been investigating nozzles formany years and it is too wide a field of activity to be fully presented in this article. However, most studies concern nozzles which have aeronautical and/or astronautical applications.

During the literature survey, a deficiency of studies in supersonic airflows which could be applied in heavy-industry equipment has attracted the authors' attention. The flow which is considered in the present case is the subject of investigation by many researchers. However, most cases of studies consider a supersonic flow in a converging-diverging nozzle and an example can be found in [1]. The authors of this article deeply investigated compressible flow through converging-diverging nozzle. The study considers experimental as well as numerical methods and their applications. The results can be very useful for a validation of numerical models, solvers and boundary conditions. The type of nozzle are injectors which were studied in [2]. Investigations of the cavitating flow at high velocities by using numerical methods are emphasized in these studies. Many papers consider flows in ejectors. Flow phenomena are reported in scientific studies [3], whereas applicable ones consider the influence of the geometry on a specific industrial application [4], [5]. The converging-diverging nozzles are still a subject for investigations due to their wide scope of application [6]. In their studies of nozzles, many authors use axisymmetric models [7] owing to their simplicity and low computational effort. Such a far-reaching simplification of the model will not be applied in this study.

The aforementioned studies are valuable with the methods and results of experiments. But they do not consider nozzles applied in heavy industry in which the flow phenomena are not obvious. The study of this type of the nozzle has been reported in [8] and there were attempts to optimize the airflow through it in 2-D [9] and 3-D [10]. The present study broadens knowledge on the supersonic flow in the channel with non-constant cross-section area where obstacles are present. The main goal of the study is to determine the amount of energy loss during the flow through the nozzle.

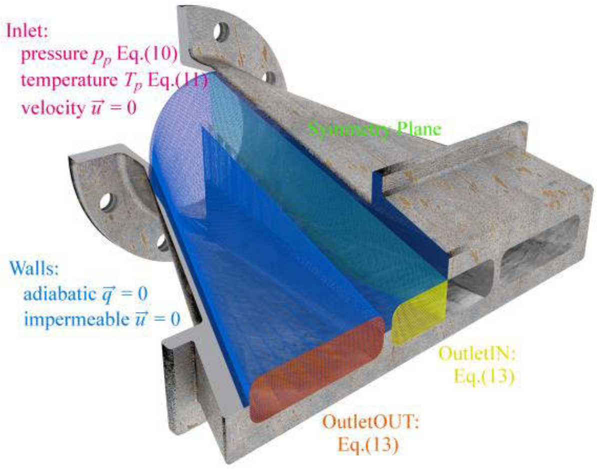

Fig. 2. Geometry model with numerical mesh visualized

2. NUMERICAL MODEL

The nozzle, which is the object investigated, is industrially applicable. The nozzle is made of cast iron with the thickness of the walls between 10 mm and 25 mm. Its visualization is shown in Figure 2. The nozzle can be attached to the pneumatic pulsator of a nominal outlet diameter 150 mm and its main dimensions are: length along the flow direction 320 mm, width: 487 mm, and height: 325 mm.

The airflow through the nozzle is driven by the difference between the internal and external pressure. The flow is transient with respect to the characteristic of pneumatic pulsator work cycle. Because of very large driving pressure difference, the flow must be considered as compressible and should be assume as super-sonic or at least trans-sonic. To calculate the unsteady compressible supersonic flow, the application *sonicFoam* is used which is part of the OpenFOAM toolbox [11]. The toolbox implements the finite volume method (FVM), one which is widely utilized in numerical simulations of fluid flows.

Air is modelled as a compressible, thermodynamically ideal gas with an invariant gas constant. For proceeding the calculations, it is convenient to assume an adiabatic flow, which is possible to do because of the very short time of the flow through the nozzle. This assumption is used for solving the governing equations.

Adiabatic flow does not exclude energy loss during airflow.

The flow domain is divided into a finite number of 1.220.569 cells what is shown in Figure 2. Inside the cells, there are flow governing equations discretized and solved which are a mathematical expression of the following laws of conservation:

– conservation of mass (continuity equation):

$$\frac{\partial \rho}{\partial t} + \nabla \cdot (\rho \vec{u}) = 0, \tag{1}$$

where: ρ is density [kg/m^3], t is time [s], and u denotes velocity of the gas [m/s],

– conservation of momentum:

$$\frac{\partial \rho \vec{u}}{\partial t} + \nabla \cdot (\rho \vec{u}\vec{u}) - \nabla \cdot \mu \nabla \vec{u} = -\nabla p, \tag{2}$$

where: μ is dynamic viscosity [Pa·s], and p denotes pressure [Pa],

– conservation of energy:

$$\frac{\partial \rho e}{\partial t} + \nabla \cdot (\rho \vec{u} e) - \nabla \cdot \left(\frac{\lambda}{C_v}\right) \nabla e = p \nabla \cdot \vec{u}. \tag{3}$$

where: e is internal energy of the gas [J/kg], λ is thermal conductivity [W/(m·K)], and C_v is specific heat at constant volume [J/(kg·K)].

For a properly stated problem, Equations (1)-(3) need to be complemented with thermodynamic relations of gas constant and internal energy as follows:

$$R = C_p - C_v = \frac{p}{\rho T} = 287 \frac{\mathrm{J}}{\mathrm{kg \cdot K}}, \tag{4}$$

$$e = C_v T, \tag{5}$$

where T denotes temperature [K] and C_p – specific heat at constant pressure [J/(kg·K)].

Furthermore, the heat conduction should also be taken into account and an appropriate conduction equation (i.e. Fourier's law) has to be added to the system of equations:

$$\vec{q} = -\lambda \nabla T. \tag{6}$$

In order to solve the aforementioned equations by using FVM, Gauss linear integration is used, which is second-order accurate, for spatial discretization. To discretize the time derivatives, an implicit Euler, first-order accurate, scheme is used.

The system of governing equations delivers proper results just for laminar flows. Pre-calculated Reynolds number is $1.5 \cdot 10^6$ for the case of the present study, and therefore, a turbulence model is needed to deliver accurate results.

For the present study, the two-equation model standard k-ε [12] has been chosen with additional equations of kinetic energy of turbulence (k), dissipation rate of this energy (ε), and turbulent viscosity (μ_t). This model is also well-validated by experimental results. From the many advantages of using this model, the most important is that the this model is suitable for the cases where the parameters of free stream are more important than the influence of the fluid onto the walls:

$$\begin{aligned} &\frac{\partial}{\partial t}(\rho k) + \nabla \cdot (\rho k \vec{u}) = \\ &= \nabla \cdot \left[\left(\mu + \frac{\mu_t}{\sigma_k}\right) \nabla k\right] + P_k - \rho\varepsilon - Y_M + S_k, \end{aligned} \tag{7}$$

$$\begin{aligned} &\frac{\partial}{\partial t}(\rho \varepsilon) + \nabla \cdot (\rho \varepsilon \vec{u}) = \nabla \cdot \left[\left(\mu + \frac{\mu_t}{\sigma_\varepsilon}\right) \nabla \varepsilon\right] + \\ &+ C_{1\varepsilon} \frac{\varepsilon}{k} P_k - C_{2\varepsilon} \rho \frac{\varepsilon^2}{k} + S_\varepsilon \qquad , \end{aligned} \tag{8}$$

$$\mu_t = \rho C_\mu \frac{k^2}{\varepsilon}, \tag{9}$$

where $C_{1\varepsilon}$ = 1.44, $C_{2\varepsilon}$ = 1.92, C_μ = 0.09, σ_ε = 1.3, σ_k = 1.0 are model constants. The values of these constants are taken from experiments, and they are well validated in practical applications [13].

In order to solve the system of governing equations, a numerical model needs to be complemented by boundary and initial conditions. Time-varying conditions are modelled by using variable inlet pressure and temperature.

Inlet data are taken from previous work [14]. Patch (boundary) pressure is calculated from the total (stagnation) pressure according to the following expression:

$$p_p = \frac{p_0}{\left(1 + \frac{\gamma - 1}{2\gamma} \psi \, |\vec{u}|^2\right)^{\frac{\gamma}{\gamma - 1}}}, \tag{10}$$

where γ = 1.4 is adiabatic index. Time-dependency between the value of stagnation and static pressure is shown in Figure 3.

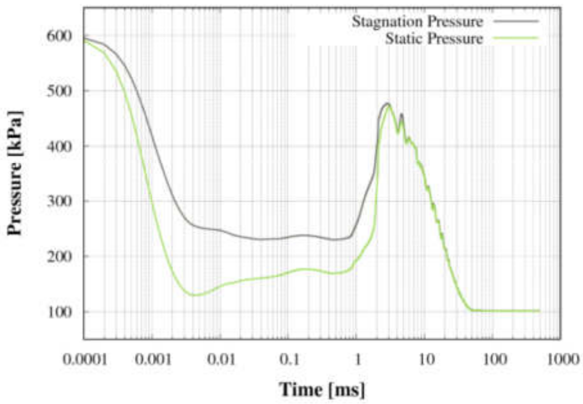

Fig. 3. Time dependency of inlet pressure

The temperature boundary condition is described similarly to the pressure one, where boundary condition is calculated from the following equation:

$$T_p = \frac{T_0}{1 + \frac{\gamma-1}{2\gamma}\psi\,|\vec{u}|^2} \tag{11}$$

and the graph of both static and stagnation temperature versus time is shown in Figure 4.

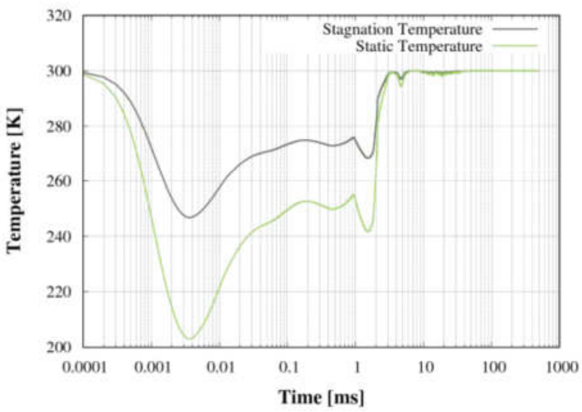

Fig. 4. Temperature dependency

Eq. (11) and (12) consist of the so-called compressibility, which is defined as follows:

$$\psi = \frac{\partial\rho}{\partial p} = \frac{1}{RT}\,. \tag{12}$$

The outlet pressure (and other terms) is calculated according to the wave transmissive boundary condition, which is of the Robin type [15], as follows:

$$\frac{\partial\phi}{\partial t} + \vec{u}\,(\vec{n}\cdot\nabla\phi) = \frac{\vec{u}}{l_\infty}\,(\phi_\infty - \phi), \tag{13}$$

where the values of outlet terms ϕ are calculated by using far field values ϕ_∞ being located in a known distance from the outlet l_∞. The wave transmissive boundary condition includes a velocity vector in its definition, and therefore, it can be regarded as a convective one. Initial values for this condition were applied at the outlet for scalar fields of pressure (p_∞ = 10^5 Pa) and temperature (T_∞ = 300 K) and for velocity vector field (u_∞ = 0 m/s). The values were obtained by using this condition are “transferred” from the outlet of the nozzle to the environment. Furthermore, it does not allow shock waves to be reflected back to the flow domain, which is possible with Neumann-type boundary conditions.

The inlet boundary conditions are Dirichlet type for scalars (pressure and temperature) and Neumann type for velocity; i.e. $\vec{n}\cdot\nabla\vec{u} = 0$.

The flow is assumed symmetrical in the numerical model and there is only one half of the nozzle analysed with the symmetry plane boundary condition applied. This condition equalizes the components of the gradients which are normal to the plane to zero; i.e. $\vec{n}\cdot\nabla\phi = 0$.

While proceeding numerical simulations, it is very important to check the error of calculations. The most procedures of the error estimation are based on the residuum value of the chosen source term.

The accuracy of the results could be determined only when an exact solution is known. The case is analytically unsolved so error estimation procedure must be applied in order to check the reliability of the results. There were additional calculations performed for the determination of the Grid Convergence Index (*GCI*). The index is calculated for coarser (GCI_C = 1.05·10^{-3}) and finer (GCI_F = 0.19·10^{-3}) mesh. The conditions of the error estimation procedure in numerical simulation have been positively fulfilled because $GCI_C > GCI_F$.

Further description of the problem can be found in [16] and practically applicable procedures can be found in [17] and [18].

3. ENERGY ANALYSIS

During an infinitely consecutive work cycle, the energy of inlet gas differs from the energy of the gas at the outlet. The difference is converted into heat which is transferred onto the wall of the nozzle. The value of energy and heat can be determined by the energy balance [19], which is obtained from the First Law of Thermodynamics as follows:

$$\dot{E} = H + L\,, \tag{14}$$

where H is the sum of heat exchanged with environment and the heat of physiochemical reactions in a time unit, and L is work exchanged with environment in a time unit.

For the purpose of the study it is convenient to present the FLT in its integral form in which the substantial derivative of energy is as follows:

$$\dot{E} = \frac{\partial}{\partial t}\int_V \rho\left(e + \frac{1}{2}\vec{u}\cdot\vec{u}\right)\mathrm{d}V + \oint_S \rho\left(e + \frac{1}{2}\vec{u}\cdot\vec{u}\right)\vec{u}\cdot\vec{n}\,\mathrm{d}S. \tag{15}$$

There are no chemical reactions during the airflow and the gas conversion is assumed adiabatic, so there is an absence of internal heat sources. Thus:

$$\dot{E} = \oint_S \rho\left(e + \frac{1}{2}\vec{u}\cdot\vec{u}\right)\vec{u}\cdot\vec{n}\,\mathrm{d}S. \tag{16}$$

Calculation of the heat is based on the mean values of source quantities (source terms) which are taken from the values at the inlet and the outlet of the nozzle. The mean values for scalar fields and vector volume fields are area weighted averages which are obtained according to the following equation:

$$\overline{\phi}_S = \frac{1}{S}\int_S \phi \, \mathrm{d}S. \tag{17}$$

The mass flux of the gas is a scalar surface field and it is influenced by the symmetry plane boundary condition. And with the assumption of the impermeability of walls, only the fluxes of the inlet and the outlet are taken into account, and the mass flux mean value is calculated as follows:

$$\dot{m} = 2\int_S \rho\vec{u}\cdot\vec{n}\mathrm{d}S. \tag{18}$$

Instantaneous energy flux at the inlet and the outlet is determined by inserting mean values from Eq. (18) to Eq. (16):

$$\dot{E} = \dot{m}\left(e + \frac{u_n^2}{2}\right), \tag{19}$$

where $u_n = \vec{n}\cdot\vec{u}$ denotes normal velocity to the boundary area.

4. RESULTS AND DISCUSSION

The flow through the nozzle is transient with large changes of flow parameters. Inlet air velocity changes from 0 to over 300m/s in less than 5μs. It is accompanied by an increase of the Mach number up to supersonic values. The highest Mach number reaches the value of about 1.7, which can be observed on the plot shown in Figure 5.

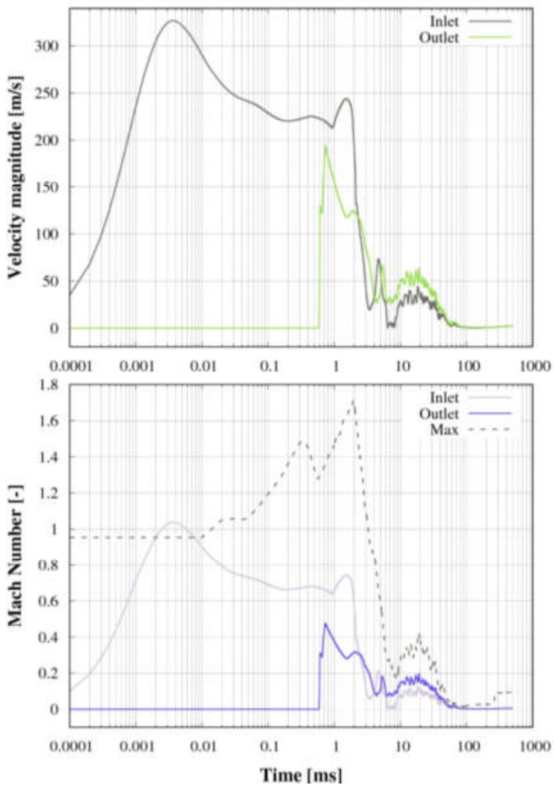

Fig. 5. Inlet and outlet velocity magnitude and Mach number

The driving force of the airflow is the pressure difference between nozzle sides. As it was mentioned before, the inlet pressure is changing in time and therefore the driving force is changing, too. Various pressure entails variability of other flow parameters such as temperature. The mean value of inlet and outlet pressure and temperature is shown in Figures 6 and 7 below. Visualization of instantaneous distribution of velocity magnitude, pressure, temperature is shown in Figure 8. All the presented contours show values at simulation time of 0.001s from the start.

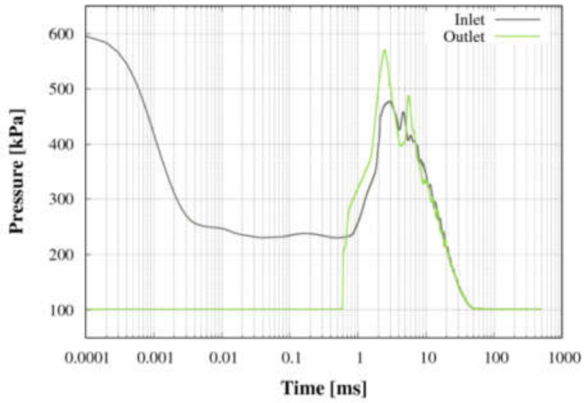

Fig. 6. Mean pressure values at inlet and outlet

The outlet temperature steeply increases up to a value of over 400K. It suggests a high level of gas compression occurrence at the nozzle outlet. The outlet pressure reaches values almost close to the highest inlet value at the same time. While the air flux reaches the nozzle outlet, the gas is initially heated, but after its maximum the temperature steeply drops to the value of 260K. This drop may cause the cooling of the loose material bed in the silo.

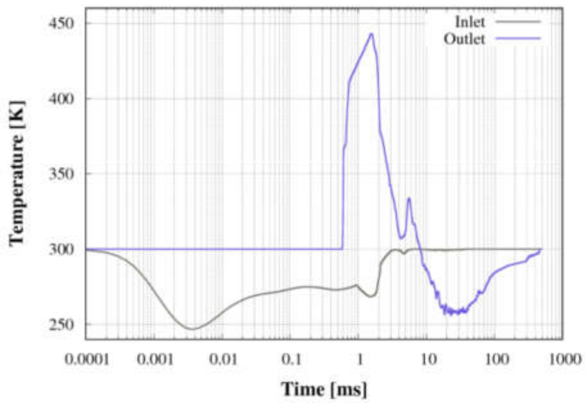

Fig. 7. Mean temperature values at inlet and outlet

Simulation results make it possible to determine the values of energy of the gas at inlet and outlet of the nozzle. They are the instantaneous values and their time distribution is shown in Figure 9. Energy itself is time independent and therefore energy fluxes are more suitable to present as time plot.

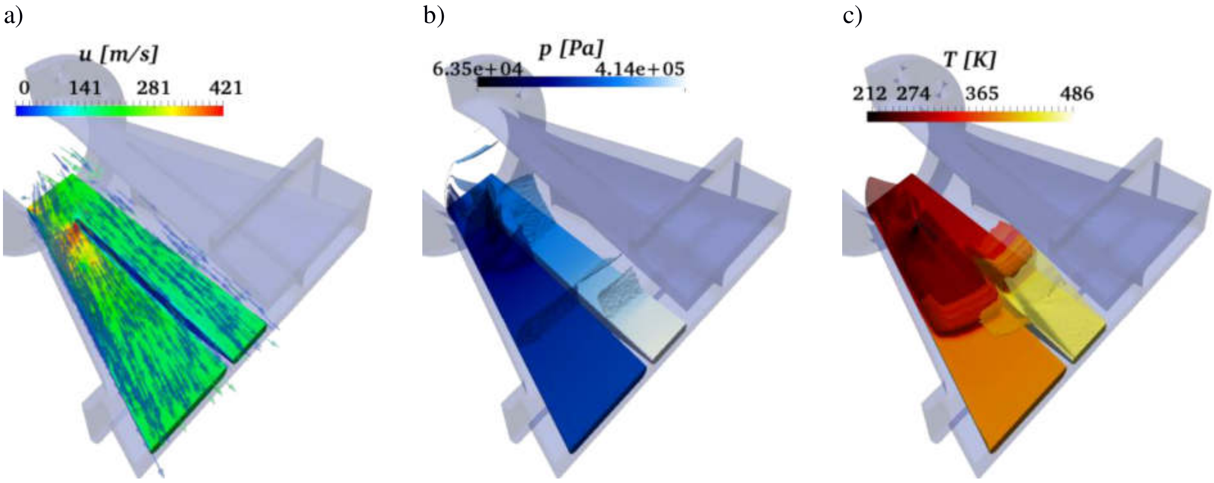

Fig. 8. Instantaneous contours of flow parameters at 1 ms of simulation time: a) velocity magnitude, b) static pressure, c) static temperature

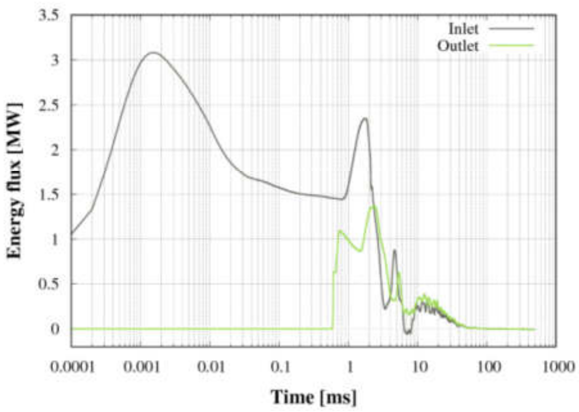

Fig. 9. Inlet and outlet energy fluxes

As it can be observed, the largest difference between the inlet and outlet energy fluxes is at the beginning of the process until the air flux reaches the outlet. At this time, the highest energy flux is over 3MW in time lapse between 1 and 2μs from the start of the simulation.

So high energy flux results are not identical with the large amount of energy of the gas. The reader must aware that the time of entire process is less than 500ms and the time in which gas flows from the inlet to the outlet of the nozzle is barely 0.6ms. Hence, the flux influences on the loose material bed for a very short time.

Non-zero energy flux at the outlet is present after simulation time of 0.6ms. The energy flux has also its local maximum after 1ms of simulation time. After that, the flux decreases with several local peaks and it reaches zero at outlet after about 60ms. The simulation has been carried out up to 500ms in order to the inlet and outlet mass fluxes give sum of zero. It has been a method to avoid abnormality in energy analysis.

The reader may have an impression that the value of inlet energy is much large at the outlet. One must aware that the x-axis is in logarithmic scale. Maximal values of energy flux are available for a small time frames of order of magnitude 10^{-6}s. Thus, for proper nozzle functioning analysis, it is necessary to obtain a total value of energy.

In order to get the information of energy losses during the whole process, the total energy must be determined. In terms of definition of the energy rate, the total energy is an integral of the energy flux over the time. The integral is switched to a sum if the discrete data are taken into account:

$$E = \int_{t_0}^{t_1} \dot{E}\, \mathrm{d}t = \sum \dot{E} \cdot \Delta t, \tag{20}$$

and the values are obtained for inlet and outlet separately.

Energy increment or loss can be calculated by using difference between inlet and outlet energy:

$$\Delta E = E_{in} - E_{out} \tag{21}$$

and it gives values of $\Delta E = 76.9\,\mathrm{J}$.

Positive value means that the total energy is larger than the energy which is transferred through the outlet of the nozzle. Thus, the results of the simulation point that the flow and the gas conversions related with it causes loss which in a result will lead to heating the walls of the nozzle. The value of energy increment related to the value of delivered energy give a small amount of loss of 0.74%.

5. CONCLUDING REMARKS

Investigation of the gas flow through the pneumatic pulsator nozzle by using numerical simulation have been done. The results of simulation made it possible to carry out the energy analysis of the flow which has been modelled as compressible and supersonic. There has been a thermodynamically ideal model of the gas applied.

Provided that the value of the temperature does not exceed 450 K, the model of the gas is not erroneous [20].

Instantaneous values of energy flux are very large, however, it is available at very short time frames. Total values of energy show that the energy loss is less than 1% of inlet energy. The loss is converted into heat, so the nozzle would be a little warmed. At the same time, the outlet gas flux is compressed firmly and by that the outlet temperature increases. Instantaneous results of simulation have indicated locally chocked flow which intensifies flow parameters in similar way the converging-diverging nozzles do.

The investigation has been aimed at developing and applying a method to calculate the energy balance during the gas conversion. The investigated subject is the nozzle which is an auxiliary equipment of the pneumatic pulsator for unclogging the outlets of the silos for loose materials. The method has been intended to use in further investigation on the other elements of the pneumatic pulsator system. The results presented in the article are obtained by using area-averaged values of outflow quantities which causes some limitations. While averaging values, the information on which part of air stream causes the largest exergy destruction is smeared. Nonetheless, the method fills the gap in exergy analysis and allows to analyse time-dependent phenomena. Furthermore, there is no need to make simplification (e.g. one-dimensional) of the model.

The method needs a large amount of data for analysis and therefore it is very difficult for direct experimental verification. Thus, it is very important to proceed a solver validation and very careful simulation preparations according to the best practices in a specific field of activity.

References

1. Quaatz, J. F., Giglmaier, M., Hickel, S., Adams, N. A. (2014). Large-eddy simulation of a pseudo-shock system in a Laval nozzle. *International Journal of Heat and Fluid Flow*, *49*(C), 108–115.
2. Yuan, W., Sauer, J., Schnerr, G. H. (2001). Modeling and computation of unsteady cavitation flows in injection nozzles. *Mécanique & industries*, *2139*, 383–394.
3. Hemidi, A., Henry, F., Leclaire, S., Seynhaeve, J. M., Bartosiewicz, Y. (2009). CFD analysis of a supersonic air ejector. Part I: Experimental validation of single-phase and two-phase operation. *Applied Thermal Engineering*, *29*(8–9), 1523–1531.
4. Lin, C., Cai, W., Li, Y., Yan, J., Hu, Y., Giridharan, K. (2013). Numerical investigation of geometry parameters for pressure recovery of an adjustable ejector in multi-evaporator refrigeration system. *Applied Thermal Engineering*, *61*(2), 649–656.
5. Zhu, Y., Cai, W., Wen, C., Li, Y. (2009). Numerical investigation of geometry parameters for design of high performance ejectors. *Applied Thermal Engineering*, *29*(5–6), 898–905.
6. Zhu, Y., Jiang, P. (2014). Experimental and analytical studies on the shock wave length in convergent and convergent-divergent nozzle ejectors. *Energy Conversion and Management*, *88*, 907–914.
7. Lee, K. H., Setoguchi, T., Matsuo, S., Kim, H. D. D. (2003). The Effect of the Secondary Annular Stream on Supersonic Jet, *17*(11), 1793–1800.
8. Wołosz, K. J., Wernik, J. (2016). On the heat in the nozzle of the industrial pneumatic pulsator. *Acta Mechanica*, *227*(4), 1111–1122.
9. Wołosz, K. J., Wernik, J. (2014). The improvement of the pneumatic pulsator nozzle according to the results of the continuous adjoint for topology optimization. *Logistyka: czasopismo dla profesjonalistów*, (6), 11007–11013.
10. Wolosz, K. J., Wernik, J. (2015). Three-dimensional flow optimization of a nozzle with a continuous adjoint. *International Journal of Nonlinear Sciences and Numerical Simulation*, *16*(3–4).
11. OpenFOAM. (2017). The Open Source Computational Fluid Dynamics (CFD) Toolbox. User Guide by OpenFOAM.
12. Menter, F. R. (1994). Two-equation eddy-viscosity turbulence models for engineering applications. *AIAA journal*, *32*(8), 1598–1605.
13. Tu, J., Yeoh, G., Liu, C. (2013). *Computational uid dynamics. A practical approach*. Amsterdam: Elsevier.
14. Wołosz, K. J. (2018). Exergy destruction in the pneumatic pulsator system during one working cycle. *Energy*, *146*, 124–130.
15. Utyuzhnikov, S. V. (2008). Robin-type wall functions and their numerical implementation. *Applied Numerical Mathematics*, *58*(10), 1521–1533.
16. Jasak, H., Gosman, A. D. (2003). Element residual error estimate for the finite volume method. *Computers & Fluids*, *32*(2), 223–248.
17. Ferziger, J. H., Peric, M. (2003). *Computational methods for fluid dynamics*. *Computers & Mathematics with Applications* (Vol. 46). Springer.
18. Freitas, C. J. (2002). The issue of numerical uncertainty. Applied Mathematical Modelling, 26(2), 237–248.
19. Szumowski, A., Selerowicz, W., Piechna, J. (1988). Gas dynamics (in Polish). Warsaw: WUT Publishing.
20. Lunev, V. (2009). *Real Gas Flows with High Velocities*. Boca Raton: CRC Press.

Biographical notes

Krzysztof J. Wołosz received his M.Sc. in Faculty of Civil Engineering, Mechanics and Petrochemistry, Warsaw University of Technology Branch in Płock. At the time being he is a researcher in Department of Process Equipment at this University. He is an expert of Association of Mechanics and Mechanical Engineers with speciality of Chemical Industry Equipment. He specializes in calculation of flow phenomena in continuous media with application in industry. He is an author and co-author of 40 scientific papers.

Jacek Wernik received his MSc in mechanical engineering 1997 and PhD 2005, from Warsaw University of Technology where he also took two postgraduate courses in Information Technology and Project Management. Participant in Framework Programs UE. Author or co-author of 40 papers published in peer-reviewed scientific journals. Since 2016 director of Institute of Mechanical Engineering.